Structural phase transitions and conduction properties of superionic, ferroelastic $Cu_6PS_5Br_{1-x}I_x$ single crystals (x = 1, 0.75, 0.5, 0.25)

2006 J. Phys.: Condens. Matter 18 4489

(http://iopscience.iop.org/0953-8984/18/19/005)

INSTITUTE OF PHYSICS PUBLISHING JOURNAL OF PHYSICS: CONDENSED MATTER

J. Phys.: Condens. Matter **18** (2006) 4489–4502 doi:10.1088/0953-8984/18/19/005

Structural phase transitions and conduction properties of superionic, ferroelastic $Cu_6PS_5Br_{1-x}I_x$ single crystals ($x = 1, 0.75, 0.5, 0.25$)

A Gągor[1,4], A Pietraszko[1], M Drozd[1], M Połomska[2], Cz Pawlaczyk[2] and D Kaynts[3]

[1] W Trzebiatowski Institute of Low Temperature and Structure Research, PAS, PO box 1410, 50-950 Wroclaw, Poland
[2] Institute of Molecular Physic, PAS, M Smoluchowskiego 17, 60-179, Poznań, Poland
[3] Uzhhorod State University, Uzhhorod, Ukraine

E-mail: a.gagor@int.pan.wroc.pl

Received 13 December 2005, in final form 30 March 2006
Published 25 April 2006
Online at stacks.iop.org/JPhysCM/18/4489

Abstract

A new concentration–temperature phase diagram of superionic $Cu_6PS_5Br_{1-x}I_x$ mixed crystals with compositions $x = 1$, 0.75, 0.5, 0.25 is proposed on the basis of calorimetric, optical and single-crystal x-ray diffraction measurements. In the high temperature form, above the first phase transition, all compounds crystallize in cubic symmetry $F\bar{4}3m$. In iodine rich crystals (for $x = 1$, 0.75 and 0.5) below 270 K intermediate cubic $F\bar{4}3c$ superstructure is stabilized down to 143–169 K for $x = 1$ and around 220 K for $x = 0.75$ and 0.5. Below these temperatures ferroelastic phase transition to monoclinic Cc phase takes place. On the other hand, in bromine rich compounds ($x = 0.25$) a direct $F\bar{4}3m$–Cc phase transition is observed without any indications of intermediate cubic superstructure. The influence of compositional disorder on superionic properties is discussed on the basis of conductivity measurements for temperatures between 150 and 290 K. Since conduction properties are coupled with the structure changes the different conductivity behaviour is observed for different I/Br concentration. Ionic conductivity decreases with the increase of bromine concentration. Even in the high temperature phase conductivity is lower and activation energy is higher in bromine rich compounds.

1. Introduction

The $Cu_6PS_5Br_{1-x}I_x$ solid solution belongs to the family of argyrodites [1]. Over the last few decades copper based argyrodites have attracted considerable interest due to their physical

[4] Author to whom any correspondence should be addressed.

properties and possible technical applications. Cu_6PS_5X (X: Cl, Br, I) are well known as ferroelastic fast ion conductors with copper Cu^+ ions as charge carriers. The original structure properties make these compounds interesting for ion-dynamics and order–disorder studies [2–6]. Here, we report the results of an investigation of the influence of compositional disorder on structure and charge transport properties in $Cu_6PS_5Br_{1-x}I_x$ solid solution. There is an important issue within a field of ionic conductors to explain the effect of chemical substitution on charge transport. Dopants may either promote or hinder superionic behaviour through modification of the anion sublattice structure.

Regarding the pure Cu_6PS_5I and Cu_6PS_5Br it was shown that in these compounds instead of dynamic structural disorder connected with copper migration static disorder occurs. It is induced by the differences in crystal preparation procedure which can enrich or impoverish crystals in copper ions. The static structural disorder has an influence on the superionic and ferroelastic phase transition (PT) in both compounds [4, 5] and seems to be the reason for discrepancies in determination of this transition temperature by different research groups [4, 6]. In $Cu_6PS_5Br_{1-x}I_x$ solid solution these two types of disorder described above are accompanied by compositional disorder.

As regards the crystal structure of Cu_6PS_5I and Cu_6PS_5Br at room temperature it was shown in [7, 8] that these compounds accommodate cubic system with the space group $F\bar{4}3m$. Cu_6PS_5Br crystals undergo ferroelastic phase transition with symmetry change from $F\bar{4}3m$ to Cc at (268 ± 2) K and isostructural superionic phase transition at $T_s = (173 \pm 7)$ K [9]. Whereas Cu_6PS_5I pure crystals undergo two structural PTs, the first at $T_1 = 274$ K with change of the symmetry to $F\bar{4}3c$ cubic superstructure (new lattice parameter $a' = 2a$), and the next one ferroelastic at $T_c = (143–169)$ K, connected with the symmetry change from $F\bar{4}3c$ to Cc [10]. The distribution of copper ions in the structure plays a major role in the observed physical behaviour. In the cubic $F\bar{4}3m$ phase copper ions are distributed statistically over many tetrahedral, triangular and linear coordination sites in the argyrodite-type framework (PS_5X). In the $F\bar{4}3c$ superstructure an ordering process in the copper sublattice is observed. Finally, monoclinic Cc phase is characterized by fully occupied copper sites. The changes in the copper sublattice influence conduction properties of these compounds. In Cu_6PS_5Br crystals the ionic conductivity is lower and activation energy is higher than that in Cu_6PS_5I [11].

In this paper we present the entire concentration–temperature phase diagram of $Cu_6PS_5Br_{1-x}I_x$ mixed crystals prepared on the basis of single-crystal x-ray diffraction, calorimetric measurements and domain structure observation. Moreover, impedance spectroscopy is applied to confront structural results with temperature and concentration changes of ionic conductivity.

2. Experimental details

The $Cu_6PS_5Br_{1-x}I_x$ single crystals were obtained by the conventional vapour transport method at the Uzhhorod State University. The DSC measurements were performed on a Perkin-Elmer DSC-7 in the temperature range 100–320 K.

Optical microscopy observations were performed under the polarizing microscope. For these studies samples were cut out from a high-quality as-grown crystal in the (001) crystallographic direction. The thickness of plates was about 0.15 mm. The thermal cycle applied to the samples was performed as follows: the sample was cooled down directly from room temperature to a temperature below T_c and then heated. The cooling and heating rate was 1 K min^{-1}. The sample was held in a Linkam cooling–heating stage and the temperature of the specimen was controlled within 0.1 K. The pictures were taken by a commercial digital camera.

Single-crystal x-ray study was performed on a Kuma KM4CCD diffractometer with graphite-monochromated Mo Kα radiation. For all samples numerical absorption correction was applied. The Crys. Alis. software version 1.170.32 (Oxford Diffraction) was used for the data processing and reciprocal space reconstruction. The structures were solved using direct methods and refined by the full-matrix least squares method using the SHELX-97 program package [12]. Diffraction data were collected in the range of 125–295 K. Low temperature was maintained with a nitrogen-gas-flow cooling system (Oxford Cryosystem Controller), $\Delta T = 0.3$ K.

The electrical conductivity measurements were performed by means of dc impedance spectroscopy using a Hewlett Packard 4191A impedance analyser in the temperature range 150–300 K. The dimensions of the sample were of order $2 \times 2 \times 0.15$ mm^3. Sample contact was achieved through conducting silver paint applied to the flat faces of the crystal samples. An impedance spectrum was generated at each data temperature throughout the frequency range 5 Hz–13 MHz.

3. Results and discussion

Below we present the results obtained from DSC, optical, x-ray and impedance measurements, which give new insights into structural properties and polymorphic phase transitions in $Cu_6PS_5Br_{1-x}I_x$ mixed crystals. We discuss the structural transformations providing high copper mobility as well as the influence of compositional disorder on superionic properties in investigated compounds.

3.1. Differential scanning calorimetry (DSC)

Figure 1(a) shows DSC runs on cooling and heating for all title compounds in the high temperature range. Figures 1(b) and (c) show DSC runs in two low temperature regions for $Cu_6PS_5Br_{0.25}I_{0.75}$, $Cu_6PS_5Br_{0.5}I_{0.5}$ and Cu_6PS_5I, respectively.

In Cu_6PS_5I three thermal anomalies are observed at temperatures 143, 160 and 274 K (cooling cycle). With regard to mixed, iodine rich compounds calorimetric measurements show that we deal at least with two transformations, one at 273.4/271 K and the second one at 211/216 K for $Cu_6PS_5Br_{0.25}I_{0.75}$/$Cu_6PS_5Br_{0.5}I_{0.5}$, whereas in $Cu_6PS_5Br_{0.75}I_{0.25}$ only one heat anomaly is observed, at 269 K. All recorded heat anomalies are associated with relatively small entropy effects ($\Delta S \sim 2 \times 10^{-2}$ J g^{-1} K^{-1} for all transitions) and are characterized by relatively high temperature hysteresis in the low temperature range ($\Delta T \sim 9$ K) and a smaller one in the high temperature range ($\Delta T \sim 4$ K). This is usually treated as evidence of a first-order phase transition.

3.2. Domain structure

One of the methods applied to detect the character of transitions observed on DSC runs was polarizing optical microscopy. The main goal of this experiment was concentrated on detecting the domain structure and their changes as a function of temperature.

3.2.1. Cu_6PS_5I. With regard to Cu_6PS_5I, two samples were measured. Sample I remained optically isotropic down to 165 K. Below this temperature a part of the sample (rectangular in shape) underwent the ferroelastic phase transition (see figure 2(a)). The domain structure on the whole sample appeared below 143 K (see figure 2(b)). During the heating the domain structure outside the rectangular frame disappeared above 152 K. The sample became optically isotropic

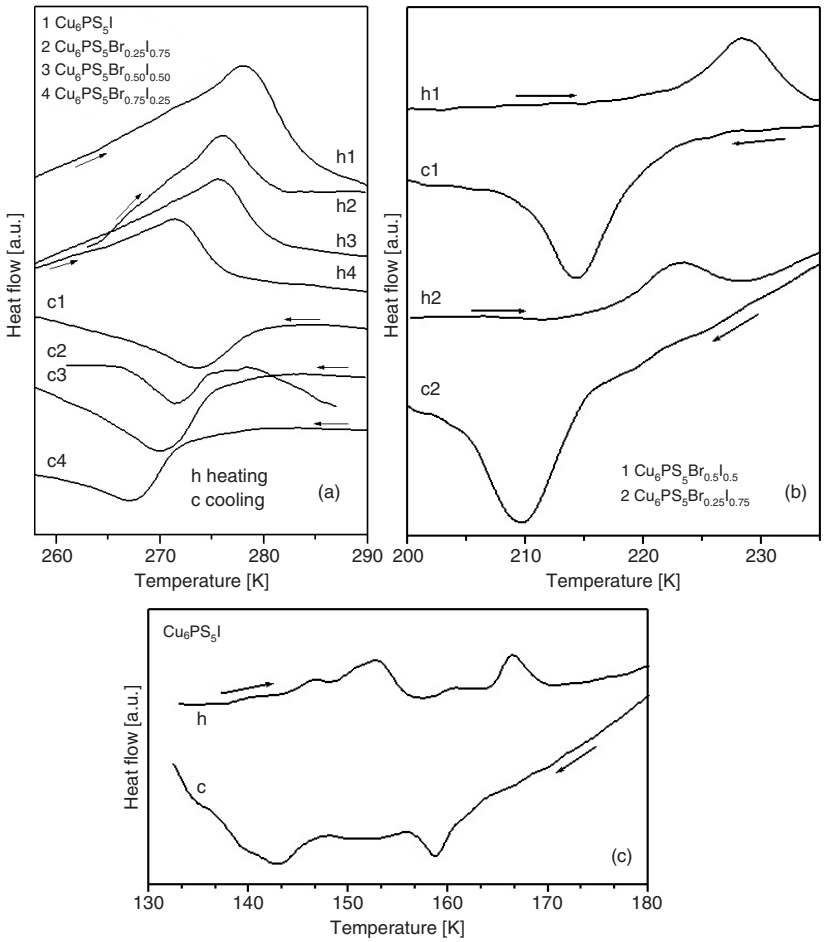

Figure 1. DSC runs on cooling and heating for (a) all compounds in the room temperature region, (b) $Cu_6PS_5Br_{0.25}I_{0.75}$ and $Cu_6PS_5Br_{0.50}I_{0.50}$ and (c) Cu_6PS_5I crystals in the low temperature region.

above 167 K. It is worth noticing that detected temperatures during the cooling and heating cycles correspond to the anomalies detected on the DSC diagram in the low temperature range.

The second sample remained optically isotropic down to 143 K. Below this temperature the sample changed colour from light to dark red and domain structure appeared, although it was not as distinct as in the case of sample I. During the heating process the crystal transformed into paraelastic phase at 150 K.

The difference in the behaviour between both samples is a consequence of the small deviation from copper stoichiometry in the measured samples. It was shown in [4, 5] that different technological procedures used in a vapour transport method result in synthesis of crystals with various copper contents. Furthermore, even small deviations from copper stoichiometry lead to different temperatures of superionic phase transition. Taking into account these results, we can infer that despite the fact that our samples were prepared under the same growth conditions seeds with different copper content were achieved. Another important fact is that the temperature of the paraelastic–ferroelastic phase transition perfectly coincides with the

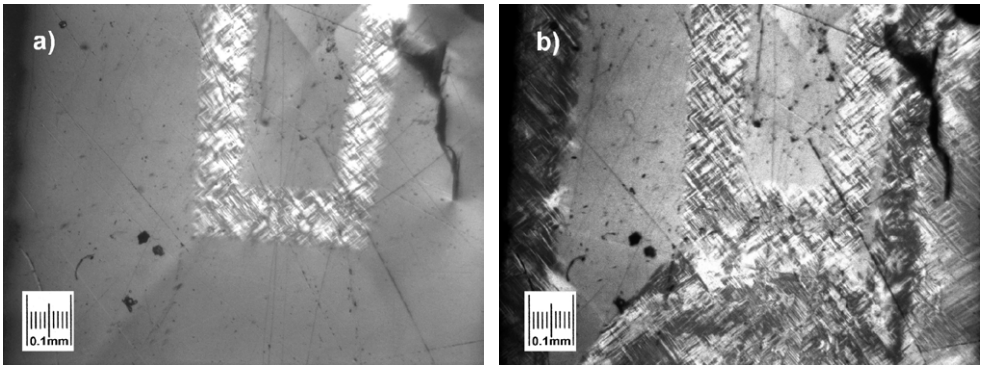

Figure 2. Domain structure in Cu_6PS_5I at (a) 165 K and (b) 143 K, sample II.

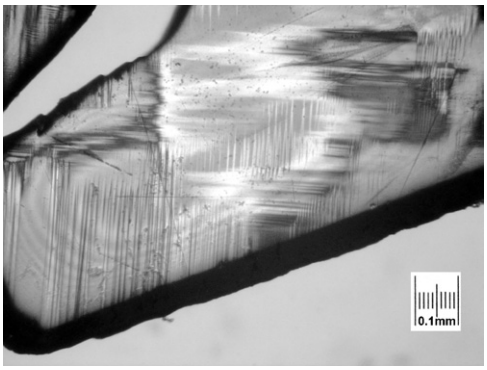

Figure 3. Domain structure in $Cu_6PS_5Br_{0.25}I_{0.75}$ at 225 K, sample II.

temperature of the superionic phase transition based on absorption edge energy reported in [4]. Therefore, we assume that in these crystals the ferroelastic phase transition is accompanied by the superionic phase transition. As a result, in Cu_6PS_5I crystals $T_c = T_s$ and only two phase transitions occur: structural at 274 K and the second one ferroelastic, superionic below 169 K.

3.2.2. $Cu_6PS_5Br_{0.25}I_{0.75}$. In the case of $Cu_6PS_5Br_{0.25}I_{0.75}$ two samples were investigated as well: sample I without any defects visible under the optical microscope, and sample II with some small cracks near the edges and impurities in the bulk. As for sample I, domain structure appeared in a part of the sample at 232 K; the whole sample underwent the transition below 225 K. During the heating it came back to the optically isotropic state at 233 K. As regards sample II, the ferroelastic domains appeared in the area of visible cracks and impurities at 253 K and started to expand all over the sample (see figure 3). At 232 K they were visible on half of the sample and finally, at 225 K, they took up the whole plate. During the heating process at 232 K half of the sample passed the transition, the other half above 242 K. The domain structure around defects remained up to 252 K.

On the basis of the experiment discussed above we could associate the broad DSC peaks in the vicinity of 211 K observed while cooling and at 220 K during the heating process with the paraelastic–ferroelastic phase transition. As in the case of Cu_6PS_5I, the temperature of this transition strongly depends on copper stoichiometry.

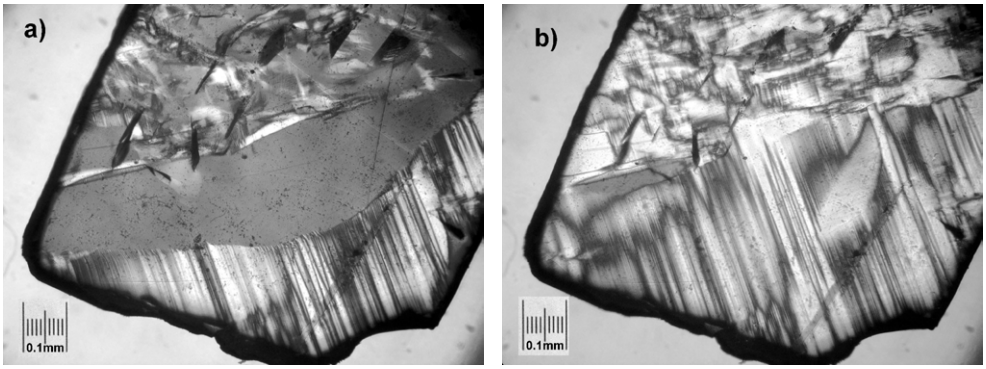

Figure 4. Domain structure in $Cu_6PS_5Br_{0.5}I_{0.5}$ at (a) 223 K and (b) 210 K.

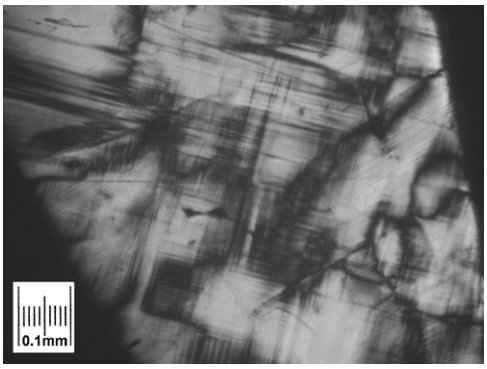

Figure 5. Domain structure in $Cu_6PS_5Br_{0.75}I_{0.25}$ at 263 K.

3.2.3. $Cu_6PS_5Br_{0.5}I_{0.5}$. Photographs of domain structure of $Cu_6PS_5Br_{0.5}I_{0.5}$ taken at 223 K and 210 K are shown in figures 4(a) and (b), respectively. The first ferroelastic domains appeared at 223 K around defects located near the edges of the plate. On further cooling we recorded jump-like transition at 210 and 206 K. At 210 K the phase front passed through part of the sample. The rest of it remained optically isotropic to the second jump at 206 K. During the heating process the phase front started moving back at 215 K. Above 225 K only vestigial domain walls were observed. The observed phenomena seem to be evidenced by DSC analysis. The broad enthalpy peaks in the vicinity of 216 K (cooling) and 235 K (heating) correspond to the paraelastic–ferroelastic phase transition.

3.2.4. $Cu_6PS_5Br_{0.75}I_{0.25}$. As regards bromine rich samples the optical changes were observed at higher temperatures. In $Cu_6PS_5Br_{0.75}I_{0.25}$, domain structure appeared at 270 K while cooling and disappeared above 272 K while heating. Furthermore, we did not observe a distinct phase front during the transition. The picture of domain structure taken at 263 K is presented in figure 5.

Summarizing, in iodine rich compound $Cu_6PS_5Br_{0.25}I_{0.75}$ the temperature of ferroelastic phase transition is increased by 80 K as compared to pure Cu_6PS_5I crystals. Moreover, higher concentration of bromine in $Cu_6PS_5Br_{0.5}I_{0.5}$ only slightly affects this temperature. Different temperatures T_c observed in different experiments are associated with static disorder connected with deviation from copper stoichiometry and poor homogeneity of the samples. This effect

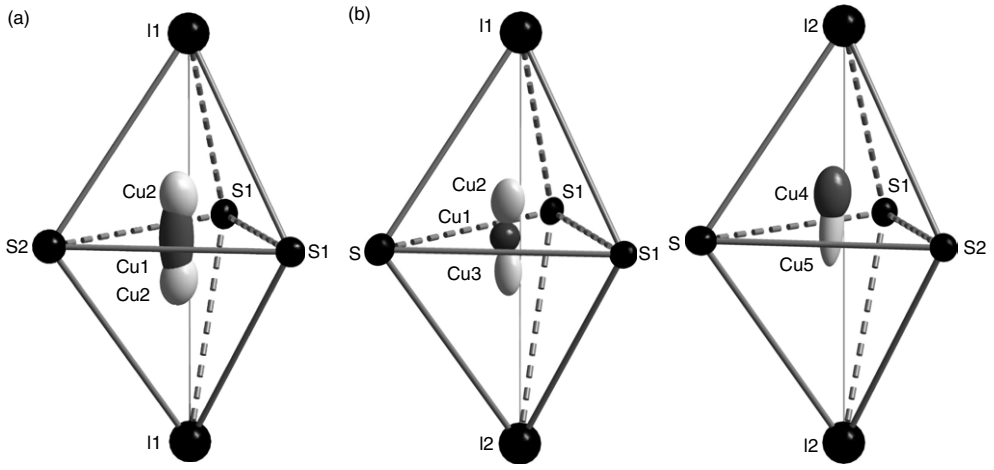

Figure 6. Coordination of copper ions in (a) $F\bar{4}3m$ phase ($T = 293$ K) and (b) $F\bar{4}3c$ phase ($T = 225$ K).

is underlined the most in the Cu_6PS_5I crystals, where T_c varies from 143 to 169 K. Moreover, it seems that the local strains speed the transition up. The domain walls appear first near the edges and cracks inside the sample.

Around 273 K in iodine rich compounds DSC runs show small anomalies. Thermal hysteresis of PTs indicate the first-order phase transitions. The lack of optical changes points to cubic–cubic phase transition.

On the other hand, in $Cu_6PS_5Br_{0.75}I_{0.25}$ only a single heat anomaly near 269 K is observed. Also in this temperature region the domain structure connected with symmetry change to the monoclinic system appears. In both experiments small thermal hysteresis is pronounced, which points to a first order phase transition. These results are similar to those observed in Cu_6PS_5Br crystals and indicate that bromine rich compounds do not exist in the intermediate phase between paraelastic cubic $F\bar{4}3m$ and ferroelastic monoclinic Cc phase.

3.3. Crystal structure

Crystallographic data and details of the structure determination of $Cu_6PS_5Br_{1-x}I_x$ are given in table 1. The x-ray studies for the title compounds performed at room temperature (RT) confirm $F\bar{4}3m$ symmetry. The crystal structure is made of a rigid ($PS_5Br_{1-x}I_x$) framework which accommodates 24 copper atoms among 72 permissible positions in the unit cell. They are located statistically at the edge of $S1(I)_4$ tetrahedra and occupy two independent 24g and 48h Wyckoff positions. The 24g position is triangularly coordinated by sulfur atoms (one S1 and two S2) while the 48h position is tetrahedrally coordinated by sulfur and iodine atoms (one S1, one I and two S2). Both triangular and tetrahedral environments are slightly deformed because copper positions are shifted from the centre toward the S1 position and the face of the tetrahedron, respectively. Figure 6(a) shows the characteristic coordination and distribution of copper in the $F\bar{4}3m$ phase in $Cu_6PS_5Br_{0.25}I_{0.75}$. At RT copper atoms make strong anharmonic vibrations along the edge of the $S1(I)_4$ tetrahedra. This, together with the relatively close vicinity of copper positions, makes it probable that jumps between them are easily thermally activated and copper atoms are able to overcome rather flat potential barrier to the neighbouring lattice site [10]. The structural data for this phase are presented in table 2.

Table 1. Experimental details.

Nominal composition	$Cu_6PS_5Br_{0.25}I_{0.75}$	$Cu_6PS_5Br_{0.25}I_{0.75}$	$Cu_6PS_5Br_{0.5}I_{0.5}$	$Cu_6PS_5Br_{0.75}I_{0.25}$
Empirical formula	$Cu_{5.79}PS_5Br_{0.21}I_{0.79}$	$Cu_{5.76}PS_5Br_{0.2}I_{0.8}$	$Cu_{5.76}PS_5Br_{0.39}I_{0.61}$	$Cu_{5.75}PS_5Br_{0.75}I_{0.25}$
Temperature (K)	225(2)	293(2)	293(2)	293(2)
Wavelength (Å)	Mo/0.710 69	Mo/0.710 69	Mo/0.710 69	Mo/0.710 69
Crystal system, space group,	cubic, $F\bar{4}3c$	cubic, $F\bar{4}3m$	cubic, $F\bar{4}3m$	cubic, $F\bar{4}3m$
Z, Pearson code	32, *cF*560	4, *cF*52	4, *cF*52	4, *cF*52
Unit cell dimensions (Å)	19.5798(23)	9.7761(11)	9.7785(11)	9.7375(11)
Volume (Å^3)	7506.3(15)	934.32(18)	935.01(18)	923.30(18)
Calculated density (g cm^{-3})	4.89	4.91	4.82	4.78
2θ range (deg)	56.5	92.51	92.48	118.75
Reflections collected/unique	3337/704	4420/450	4350/443	9615/719
R (int)	0.029	0.032	0.052	0.073
Data/restraints/parameters	704/0/65	449/0/22	442/0/22	719/0/22
Goodness of fit on F2	1.001	0.991	1.197	0.903
R_1/wR_2 [$I > 2\sigma(I)$]	0.023/0.0421	0.0231/0.0321	0.0245/0.0645	0.0373/0.0803
R_1/wR_2 (all data)	0.0434/0.0462	0.031 30/0.0330	0.0274/0.0656	0.0513/0.0860
Extinction coefficient	0.000 061(2)	0.0242(3)	0.0225(8)	0.0058(4)

Table 2. Atomic parameters of $Cu_6PS_5Br_{0.25}I_{0.75}$ at RT.

Atom	Wyckoff position	Site symmetry	x	y	z	U_{iso}	Sof.
I	*4a*	*−43m*	0	0	0	0.015 49(16)	0.799(4)
Br	*4a*	*−43m*	0	0	0	0.038(2)	0.201(4)
P	*4b*	*−43m*	0	0	0.5	0.008 98(17)	1
S1	*4d*	*−43m*	0.25	0.25	0.75	0.017 56(19)	1
S2	*16e*	*.3m*	0.378 61(4)	0.378 61(4)	0.378 61(4)	0.012 59(10)	1
Cu1	*24g*	*2.mm*	0.25	0.25	0.976 99(7)	0.053 8(3)	0.595(2)
Cu2	*48h*	*..m*	0.198 73(12)	0.301 27(12)	0.518 86(14)	0.026 8(4)	0.1816(12)

With temperature lowering, an ordering process in the copper sublattice is observed. In Cu_6PS_5Br crystals it is an sudden process connected with the change of the symmetry to the monoclinic *Cc* system at 268 K and twinning of the sample [9]. As regards Cu_6PS_5I crystals it was shown in [10] that the process of copper ordering proceeds in a continuous way. At 274 K the Cu_6PS_5I pure crystals undergo structural phase transition to a cubic superstructure. The lattice parameter doubles ($a = 19.5033$ Å at 165 K) and the symmetry changes to $F\bar{4}3c$. The axis doubling is connected with increment of independent crystallographic sites for copper atoms. In the new phase six independent copper positions with different occupancy factors are provided. With temperature decrease, copper ions start to occupy the most stable tetrahedral and triangular sites. As a result, at 165 K only three symmetry independent copper positions are occupied. Consequently, complete ordering of copper atoms at lower temperature can be at the origin of the last superionic, ferroelastic phase transition at $T_c = (143–169)$ K, connected with the symmetry change from $F\bar{4}3c$ to monoclinic *Cc* with lattice parameters $a = 11.9430(13)$, $b = 6.8890(7)$, $c = 11.9463(11)$ and $\beta = 109.458(9)$ (at 125 K).

Our low temperature single-crystal x-ray study shows that in iodine rich compounds, namely $Cu_6PS_5Br_{0.25}I_{0.75}$ and $Cu_6PS_5Br_{0.5}I_{0.5}$, intermediate $F\bar{4}3c$ superstructure occurs below 273 K. After the transition the lattice parameter doubles and at 225 K is equal to 19.5798(23) for $Cu_6PS_5Br_{0.25}I_{0.75}$. Consequently, volume increases from 934 to 7506 Å^3 and Z value from

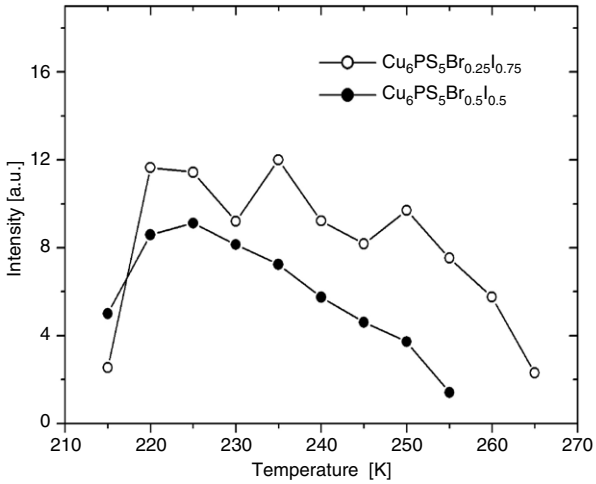

Figure 7. Integrated intensity of Bragg peak characteristic for cubic superstructure $F\bar{4}3c$ in the range of 210–270 K.

Table 3. Atomic parameters of $Cu_6PS_5Br_{0.25}I_{0.75}$ at 225 K.

Atom	Wyckoff position	Site symmetry	x	y	z	U_{iso}	Sof.
I1	*8a*	*23.*	0	0	0	0.0074(5)	0.780(6)
Br1	*8a*	*23.*	0	0	0	0.059(7)	0.220(6)
I2	*24c*	*–4..*	0.25	0.25	0	0.0086(2)	0.798(3)
Br2	*24c*	*–4..*	0.25	0.25	0	0.059	0.202(3)
P1	*8b*	*23.*	0.25	0.25	0	0.0032(8)	1
P2	*24d*	*–4..*	0.25	0	0	0.0032(8)	1
S	*32e*	*.3.*	0.125 78(6)	0.125 78(6)	0.125 78(6)	0.0136(3)	1
S1	*96h*	*1*	0.310 86(6)	0.062 08(5)	0.059 29(5)	0.0140(3)	1
S2	*32e*	*.3.*	0.310 76(6)	0.189 24(6)	0.189 24(6)	0.0104(2)	1
Cu1	*96h*	*1*	0.125 8	0.122 5	0.012 9	0.014	0.41
Cu2	*96h*	*1*	0.102 97(13)	0.101 46(13)	0.010 88(11)	0.0206(7)	0.281(2)
Cu3	*96h*	*1*	0.146 55(14)	0.143 27(14)	0.009 97(12)	0.0188(7)	0.264(2)
Cu4	*96h*	*1*	0.240 03(8)	0.150 32(7)	0.100 61(7)	0.0270(3)	0.579(2)
Cu5	*96h*	*1*	0.239 58(11)	0.129 39(13)	0.119 94(14)	0.0368(7)	0.386(3)

4 to 32. Although the Bragg peaks connected with this phase had relatively low intensity, we were able to refine the structure of $Cu_6PS_5Br_{0.25}I_{0.75}$ at 225 K. The results are presented in table 3. Figure 6(b) shows the copper coordination and copper distribution in $Cu_6PS_5Br_{0.25}I_{0.75}$ in $F\bar{4}3c$ phase. At 225 K the number of symmetry independent copper positions is equal to five.

The low temperature border of existence of this phase was determined by intensity measurements of Bragg peaks connected with $F\bar{4}3c$ superstructure (see figure 7). For both compounds it was equal to 215 K. It is not surprising taking into account the fact that higher bromine concentration in $Cu_6PS_5Br_{0.5}I_{0.5}$ almost does not change the lattice parameters and volume at RT compare with $Cu_6PS_5Br_{0.25}I_{0.75}$. Therefore, it probably has only a slight influence on changes in the copper sublattice which are substantial from the viewpoint of the observed ferroelastic phase transition. It is also worth noticing that observed temperatures of PTs

Table 4. The temperatures of structural phase transitions in $Cu_6PS_5Br_{1-x}I_x$ crystals obtained by different experimental techniques; ionic conductivity at room temperature.

	Cu_6PS_5I	$Cu_6PS_5Br_{25}I_{0.75}$	$Cu_6PS_5Br_{0.50}I_{0.50}$	$Cu_6PS_5Br_{0.75}I_{0.25}$	Cu_6PS_5Br
		T_1			
	274/277 K	273/277 K	273/277 K		
DSC		T_c		$T_1 = T_c =$	$T_1 = T_c = 268$ K
(cooling/	(143–160) K/	211/220 K	216/235 K	269/273 K	[9]
heating)	(154–167) K				
X-ray	143 K (c)	215 K (h)	210 K (h)	—	—
Domain	(143–165) K	(225–232) K	(206–210) K	270 K	—
structure					—
σ at RT	1.45×10^{-4} S cm^{-1}	5.87×10^{-5} S cm^{-1}	—	3.78×10^{-6} S cm^{-1}	$\sim 5 \times 10^{-6}$ S cm^{-1} [11]

correspond to results obtained from the DSC and optical observations. The small differences between them are probably also connected with static disorder in the samples.

In bromine rich compounds $Cu_6PS_5Br_{0.75}I_{0.25}$ the intermediate $F\bar{4}3c$ phase was not observed. Intensity measurements indicate direct $F\bar{4}3m$–Cc transition as in Cu_6PS_5Br crystals. Because of the twinning of the samples in Cc phase we were not able to refine the structures in monoclinic system.

Considering the symmetry change observed in $Cu_6PS_5Br_{1-x}I_x$ solid solution it follows that all phase transitions are first-order ones. Neither cubic $F\bar{4}3c$ nor monoclinic Cc phase is an equitranslational subgroup of cubic $F\bar{4}3m$ phase [13]. The character of these transitions is also confirmed by thermal hysteresis observed on DSC and domain structure data. Table 4 summarizes the observed temperatures of structural phase transitions obtained in different experimental techniques.

3.4. Impedance spectroscopy

There were two purposes of these measurements. Firstly, we wanted to establish the influence of the structural phase transitions on conduction properties of the crystals. Secondly, it was interesting to measure the connection between the chemical disorder and conductivity behaviour.

The dc electrical conductivity of the crystals was determined using the impedance spectroscopy method in a frequency range 5 Hz–13 MHz. An example of complex impedance measurement for $Cu_6PS_5I_{0.5}Br_{0.5}$ at room temperature is shown in figure 8. On the $Z''(Z')$ plot (Argand plot) the measuring points lie on two semicircles well separated from each other. This means that the electrical properties of the measured sample can be described by an equivalent circuit containing two parallel sub-circuits connected in series and consisting of (figure 8) (1) resistance R_b and capacity C_b (for higher frequencies) and (2) resistance R_s and capacity C_s (for lower frequencies) [14]. The first, high frequency semicircle corresponds to the bulk resistance R_b and capacitance C_b of the sample. The second, low frequency circuit originates from the electrode layer properties. The bulk conductivity σ of the sample can be determined from the bulk resistance R_b ($\sigma = d/R_bS$; d and S are the thickness and surface of the sample, respectively). The bulk resistance R_b can be obtained as a fit parameter by the fitting procedure using the formula describing the frequency dependence of the complex impedance Z^* of the whole equivalent circuit:

$$Z^*(\omega) = \frac{R_b}{1 + (i\omega R_b C_b)^{(1-\alpha_1)}} + \frac{R_s - R_b}{1 + (i\omega R_s C_s)^{(1-\alpha_2)}}, \tag{1}$$

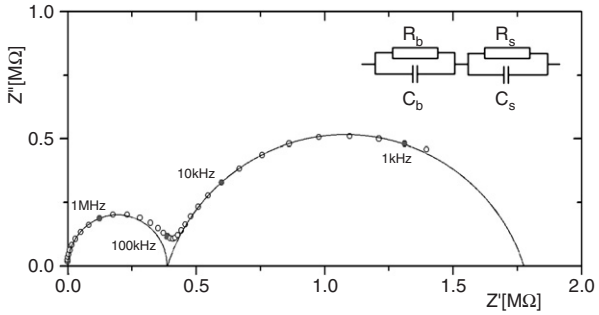

Figure 8. Typical Argand plot for $Cu_6PS_5Br_{0.5}I_{0.5}$ at room temperature. The equivalent circuit for the sample with the Argand plot is shown in inset.

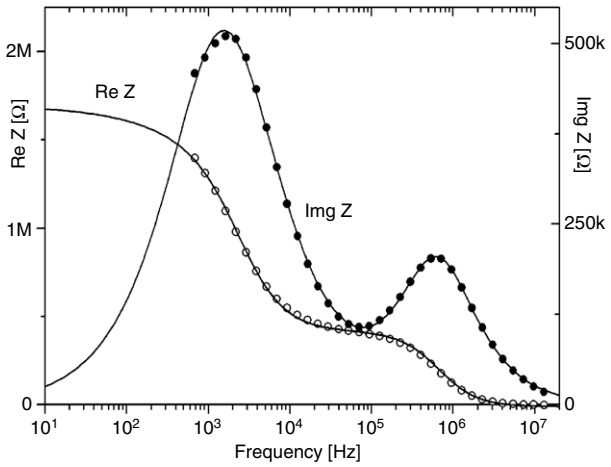

Figure 9. Frequency dependence of the real and imaginary parts of impedance in $Cu_6PS_5Br_{0.5}I_{0.5}$. The solid line was obtained by fitting the experimental points with formula (1).

where ω is the angular frequency of the measuring electrical field, α_1 and α_2-parameters describing the distribution of the time constants R_bC_b and R_sC_s in the bulk and surface layer regions, respectively. An example of such a fit for the data from figure 8 for both the real Z' and the imaginary Z'' parts of the complex impedance Z^* ($Z^* = Z' - iZ''$) is shown in figure 9. The solid lines in figures 8 and 9 were obtained by fitting the experimental data with the formula (1).

In order to determine activation energies for cation mobility in each sample the temperature dependent conductivity values were fitted to the Arrhenius law:

$$\sigma T = \sigma_0 \exp(-\Delta U/kT) \tag{2}$$

where σ_0 and ΔU denote the pre-exponential factor and the activation energy, respectively, and k is the Boltzmann constant.

The temperature dependent conductivity of measured compounds is provided in figure 10. Although the effects are subtle, in the case of Cu_6PS_5I crystals two anomalies on the Arrhenius plot can be observed. The first one at 275 K and the second one near the 235 K. The first drop in conductivity corresponds to phase transition from disordered high temperature cubic phase ($F\bar{4}3m$) to cubic superstructure ($F\bar{4}3c$). The temperature at which the second anomaly in the

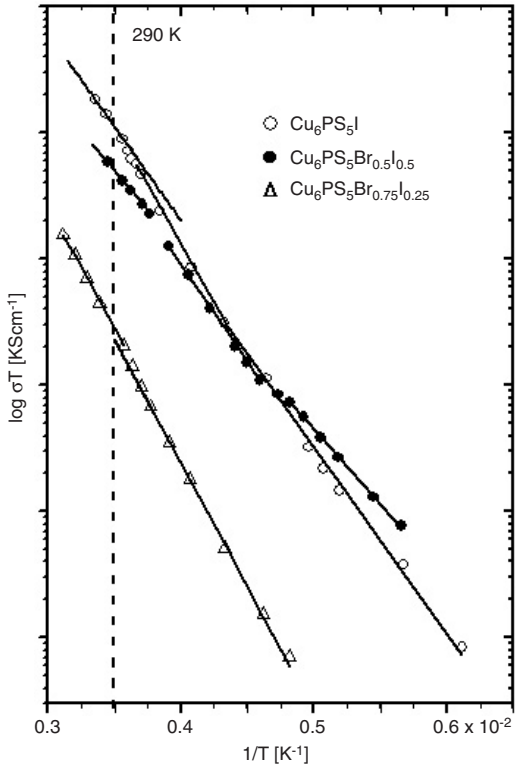

Figure 10. Arrhenius plots of the (a) Cu_6PS_5I, (b) $Cu_6PS_5Br_{0.5}I_{0.5}$ and (c) $Cu_6PS_5Br_{0.75}I_{0.25}$ argyrodites in the temperature range 150–300 K.

Arrhenius plot occurs is unrelated to the temperature of any anomaly in the x-ray diffraction and DSC curve which excludes the phase transition. Moreover, it appears in the range of cubic superstructure. This non-Arrhenius behaviour of conductivity is relatively common in the argyrodite family. It was observed in the case of Ag_7GeSe_5I [15] and $RbAg_4I_5$ [16] superionic conductors. Furthermore, it has already been reported for powder Cu_6PS_5I samples in [11] and the detailed origin of this behaviour has been described in [10]. In short, it indicates changes in conduction mechanism. Above room temperature the conductivity exceeds its value by one order of magnitude higher compared to the data reported for powder samples. The observed activation energy is also smaller ($\Delta U = 0.30$ eV) than those reported previously.

Similar behaviour in mixed crystals is observed. In $Cu_6PS_5Br_{0.5}I_{0.5}$ the Arrhenius plot can be divided into three linear regions of different activation energy. This time the temperatures at which total conductivity changes correspond to the temperatures of structural phase transitions. The upper linear region is associated with the fully disordered $F\bar{4}3m$ phase. The intermediate region is associated with cubic superstructure $F\bar{4}3c$ and the last one, in the low temperature range, is connected with ferroelastic, monoclinic Cc phase.

In bromine rich crystals there is no evidence of intermediate $F\bar{4}3c$ phase. Only a single drop in conductivity is observed near 275 K. Below this temperature the conductivity exhibits purely Arrhenius behaviour with no evidence of any electrical phase transition, which is in agreement with x-ray and DSC observations. The activation energies do not differ much before and after transition. Taking into account the static and compositional structural disorder as well

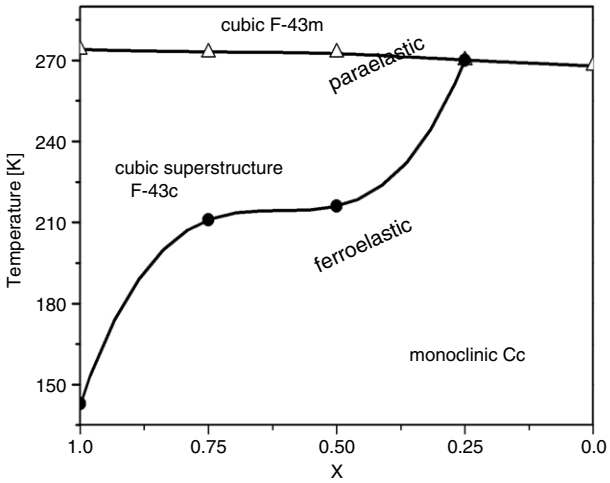

Figure 11. (X, T) phase diagram of $Cu_6PS_5Br_{1-x}I_x$ solid solution.

as experimental conditions our conductivity values differ insignificantly from those reported for Cu_6PS_5Br powder samples [11].

4. Conclusions

Connected with copper ion mobility, the properties of $Cu_6PS_5Br_{1-x}I_x$ change at various temperatures, resulting in different phases with varied characteristics. Owing to adoption of four complementary experimental techniques, DSC, optical measurements, single-crystal x-ray diffraction and impedance spectroscopy, we were able to construct a new concentration–temperature diagram of this highly disordered solid solution (see figure 11).

Summarizing, the paraelastic room temperature phase of $Cu_6PS_5Br_{1-x}I_x$ mixed crystals is characterized by a disordered copper sublattice and high ionic conductivity. With temperature lowering in iodine rich compounds the intermediate cubic superstructure is stabilized. This phase is induced by partial ordering of the copper sublattice. In bromine rich compounds it is not observed. As a result, in this crystal direct cubic–monoclinic phase transition from disordered to ordered copper sublattice occurs. Consequently, the ionic conductivity of these compounds is lower compared to iodine rich crystals.

Acknowledgments

We gratefully thank V V Panko for the crystal preparation and A Pawłowski for the sample preparation for impedance spectroscopy measurements.

This work was supported by the Polish State Committee for Scientific Research (project register 3 T08A 079 27).

References

[1] Kuhs W F, Nitsche R and Scheunemann K 1976 *Mater. Res. Bull.* **11** 1115
[2] Studenyak I P, Stefanovich V O, Kranjcec M, Desnica D I, Azhnyuk Yu M, Kovacs Gy Sh and Panko V V 1977 *Solid State Ion.* **95** 221

[3] Kranjcec M, Studenyak I P, Bilanchuk V V, Dyordyay V S and Panko V V 2004 *J. Phys. Chem. Solids* **65** 1015
[4] Studenyak I P, Kranjcec M, Kovacs Gy Sh, Panko V V, Mitrovcij V V and Mikajlo O A 2003 *Mater. Sci. Eng.* B **97** 34
[5] Studenyak I P, Kranjcec M, Kovacs Gy S, Panko V V, Azhnyuk Yu M, Desnica D I, Borets O M and Voroshilov Yu V 1998 *Mater. Sci. Eng.* B **52** 202
[6] Girnyk I, Kaynts D, Krupych O, Martunyuk-Lototska I and Vlokh R 2003 *Ukr. J. Phys. Opt.* **4** 147
[7] Kuhs W F, Nitsche R and Scheunemann K 1978 *Acta Crystallogr.* B **34** 64
[8] Nigles T and Pfitzner A 2005 *Z. Kristallogr.* **220** 281
[9] Haznar A, Pietraszko A and Studenyak I P 1999 *Solid State Ion.* **119** 31
[10] Gagor A, Pietraszko A and Kaynts D 2005 *J. Solid State Chem.* **178** 3366
[11] Beeken R B, Garbe J J and Petersen N R J 2003 *J. Phys. Chem. Solids* **64** 1261
[12] Sheldric G M 1977 SHELX-97 Program for crystal structure determination University of Cambridge, Cambridge, UK
[13] Janovec V and Kopsky V 2003 *International Tables for Crystallography D* (London: Kluwer–Academic)
[14] Macdonald J R 1987 *Impedance Spectroscopy* (New York: Wiley)
[15] Belin R, Aldon L, Zerouale A, Belin C and Ribes M 2001 *Solid State Sci.* **3** 251
[16] Zerouale A, Cros B, Deroide B and Ribes M 1988 *Solid State Ion.* **28–30** 1317